In Vivo ^{31}P MRS Study of Altered Intracellular NAD Content and NAD$^+$/NADH Redox State in Hypoxic Brain

Ming Lu[1], Xiao-Hong Zhu[1], Yi Zhang[1], and Wei Chen[1]

[1]*Center for Magnetic Resonance Research, University of Minnesota Medical School, Minneapolis, Minnesota, United States*

Introduction Nicotinamide adenine dinucleotide (NAD) participates in various redox reactions in living organisms for supporting normal cellular functions and activities (1). The reduced (NADH) and oxidized (NAD$^+$) forms of NAD convert between each other and play key roles in cellular metabolism and regulation. The intracellular NAD$^+$/NADH ratio, defined as intracellular redox state (RX), reflects metabolic status and has been found to be associated with alterations in physiology and pathology, such as aging, diabetes and cancer (2). However, direct quantification of NAD and redox state *in vivo* is challenging due to the absence of reliable approaches. Recently, we developed a novel ^{31}P MRS-based method for non-invasive quantification of NAD$^+$ and NADH contents *in vivo*, which has demonstrated the feasibility of identifying and quantifying ^{31}P MR signals of NAD$^+$ and NADH in animal brains at high magnetic field (3). In this study, to further investigate the sensitivity of this method in response to changes in energetic metabolism, alterations of the NAD concentrations and redox state in rat brains from normoxia to hypoxia were studied at 16.4 T.

Method Five male Sprague Dawley rats (BW=365±44 g) were anesthetized with 2% isoflurane in a mixture of O_2 and N_2O gases and scanned multiple times under different oxygen supply levels. For each rat, inhaling oxygen level was switched from normoxia (30~40% oxygen, baseline) to 10% (hypo_10%, 18 min), followed by ~1 hour normoxia for recovery (post) and secondary hypoxia with 5~6% oxygen (hypo_5~6%, 18 min). All MR measurements were conducted at 16.4 T/26 cm horizontal animal scanner (Varian/VNMRJ) using ^{1}H/^{31}P surface coil. Sequential ^{31}P chemical shift imaging (CSI) data of rat brains were acquired with 87 μL nominal resolution and 18 min acquisition time during the whole procedure of experiment until brain dying. A novel quantification method capable of determining the concentrations of NAD$^+$ and NADH (3) was applied. Using baseline α-ATP concentration of 2.8 mM as an internal reference (4), the absolute contents of NAD$^+$, NADH and α-ATP in each rat brain under different conditions can be measured, along with the NAD$^+$/NADH ratio and the total NAD concentration ([NAD$^+$]+[NADH]).

Results Figure 1A displays representative 3D ^{31}P CSI data of rat brain (selected chemical shift region from -9 to 11.5 ppm, referenced to phosphocreatine at -2.5 ppm), including spectra from individual voxels. At ultrahigh field, improved sensitivity and spectral quality ensured reliable quantification of cerebral NAD contents and redox states. Figure 1B demonstrated the original and fitted ^{31}P spectra of a representative rat brain under baseline, hypo_10%, post recovery, hypo_5~6% and postmortem conditions. All the resonance signals of NAD$^+$, NADH and α-ATP were satisfactorily fitted, as reflected by the small residues between the original spectra and model fittings. As shown in Figure 1B, the signal alterations of α-ATP, NAD$^+$ and NADH in response to different oxygen availabilities were clearly evident. As summarized in Figure 2, when compared with baseline, decreasing oxygen supply to 10% did not significantly change the cerebral levels of α-ATP, NAD$^+$, NADH and the redox state, which indicated a fairly sufficient oxygenation. Spectra obtained at 1 hour after the recovery of normal oxygen supply (post) demonstrated similar results as those in baseline. However, when reducing the oxygen supply to the level of 5~6% (confirmed by arterial blood gas measurements of pO_2 declining from 158±26 mmHg at baseline to 37±3 mmHg), a decrease of α-ATP was in company with NAD$^+$ reduction (-26%) and NADH increase (+25%), resulting in significant decreases in the NAD$^+$/NADH ratio (-43%) and the total NAD content (-13%). The ATP was completely depleted in the dead brain, while further increase in the NADH content and decreases in the [NAD$^+$], the NAD$^+$/NADH ratio and the total [NAD] were also observed in the postmortem brains. All of these changes are consistent as expected based on known biochemistry occurring at hypoxic condition.

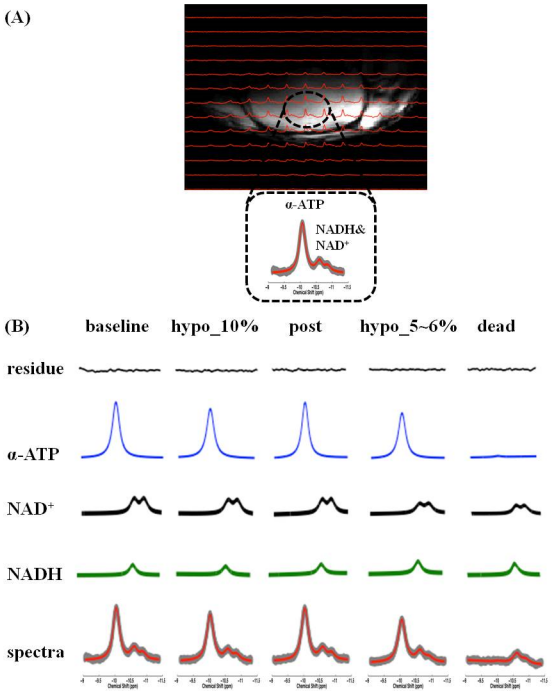

Figure 1. ^{31}P MRS of NAD in normal and hypoxic rat brain. (A) Representative ^{31}P CSI slice in transverse orientation extracted from 3D-CSI data was overlaid on corresponding anatomical image. Spectra from circled voxels were summed, enlarged and displayed to show excellent spectral quality of α-ATP, NAD$^+$ and NADH. (B) ^{31}P spectra (gray trace) and their corresponding fittings (red trace), and model decomposed individual signals of NADH (green), NAD$^+$ (black) and α-ATP (blue) obtained in a representative rat brain under different conditions.

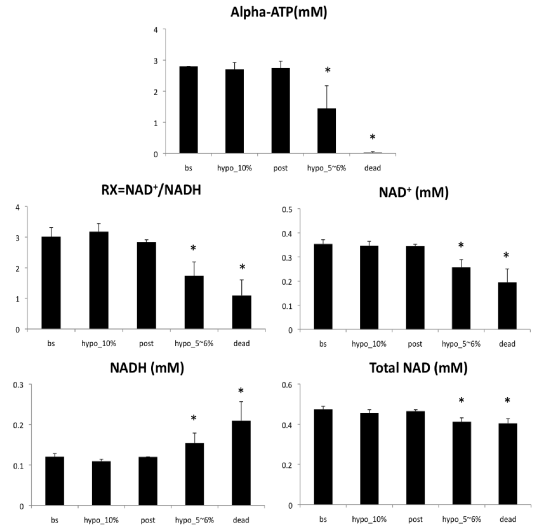

Figure 2. Summary of α-ATP, NAD contents and redox states (RX) in rat brains under different conditions (n=5, *significant difference from baseline, p<0.01 based on t-test).

Conclusion By using the novel ^{31}P MRS method alterations of the cerebral redox state and the intracellular NAD contents can be robustly and non-invasively quantified under normal and hypoxic conditions. This simple and highly applicable MR imaging approach has a great potential for studying metabolic disorders in different organs of patients with hypoxic or ischemic syndrome.

Acknowledgement NIH grants NS41262, NS57560, NS70839, P41 RR008079, P41 EB015894, P30 NS076408, S10 RR025031; Keck foundation.

References (1) Berger, F., et al. (2004) *Trends Biochem Sci.* 29, 111-118. (2) Ying, W. H. (2006) *Front Biosci.* 11, 3129-3148. (3) Lu, M., et al. (2013) *Magn Reson Med.* [Pubmed ID#23843330, Epub ahead of print]. (4) Zhu, X. H. (2009) *ISMRM* p. 4287